

Structural phase transitions of vortex matter in an optical lattice

H. Pu¹, L. O. Baksmaty², S. Yi¹, and N. P. Bigelow²

¹*Department of Physics and Astronomy, and Rice Quantum Institute, Rice University, Houston, TX 77251-1892*

²*Department of Physics and Astronomy, and Laboratory for Laser Energetics, University of Rochester, Rochester, NY 14627*

(Dated: October 16, 2018)

We consider the vortex structure of a rapidly rotating trapped atomic Bose-Einstein condensate in the presence of a co-rotating periodic optical lattice potential. We observe a rich variety of structural phases which reflect the interplay of the vortex-vortex and vortex-lattice interactions. The lattice structure is very sensitive to the ratio of vortices to pinning sites and we observe structural phase transitions and domain formation as this ratio is varied.

PACS numbers: 03.75.Mn, 03.75.Nt

Structural phase transitions (SPTs) occur in a wide range of physical and chemical systems [1]. Studies of SPTs are both of technological importance and of fundamental interest. Technologically, an understanding of SPTs is essential to the study of many materials; while fundamentally, SPTs are related to a variety of questions in statistical mechanics, crystallography, magnetism, surface science, to name a few. Among the most intensively studied systems related to SPTs are graphite intercalation compounds, niobates, adsorbed molecular monolayers and vortex matter in type-II superconductors. In this Letter we introduce a new system for SPT study: that of vortex matter created in a trapped Bose-Einstein condensate (BEC) formed in the presence of a co-rotating optical lattice (OL). This system has the advantage of being experimentally realizable, tunable over a wide range of interaction parameters, and describable by an analytic *ab initio* theory.

We take inspiration from two recent developments in atomic BECs. The first is the observation of vortex lattice excitations in rapidly rotating BECs [2]. The second is the set of proposals and demonstrations concerning periodic optical lattice potentials created using holographic phase plates [3] or amplitude masks [4]. This latter technique means that a rotating OL (at desired angular frequency) can be realized by simply rotating the OL phase plates or masks. The amenability of BECs to imaging, experimental control and theoretical description makes the atomic condensate an attractive test bed for many phenomena frequently encountered, but often difficult to study in other systems. One such example is given by the recent spectacular realization of the superfluid-Mott insulator quantum phase transition in a condensate confined by an optical lattice [5] following a proposal of Jaksch *et al.* [6]. This transition was theoretically predicted over a decade ago [7] in the context of liquid ⁴He absorbed in porous media.

In our system, the phase transition is observed as a shift in the periodicity and symmetry of the vortex lattice as optical potential parameters are tuned. Fundamentally, this situation is analogous to that of a type-II superconductor subject to external magnetic field and artificial periodic pinning [8, 9, 10]. In the analogy, the angular rotation $\Omega\hat{z}$ of the BEC plays the role of the

magnetic field and the peaks of the OL play the role of the pinning centers. In contrast to the pinning lattice in typical superconducting samples, the periodicity and depth of the optical lattice may be dynamically tuned in an atomic system. Furthermore, the clean microscopic physics of atomic condensates makes a first principles calculation possible based on a mean-field treatment. This is in contrast to the superconductor case, where theoretical calculations frequently rely on elegant, but phenomenological models or molecular dynamics simulations [9].

We work in a pancake shaped geometry. For the BEC, this is justified because at high rotation rates, the centrifugal forces reduce the radial trapping frequency ω_{\perp} and the condensate may be accurately assumed to be frozen into the harmonic oscillator ground state in axial direction (\hat{z}). We therefore integrate the axial degree of freedom, obtaining an effective two-dimensional system with a renormalized coupling constant. In a frame rotating with angular velocity $\Omega\hat{z}$ the transverse wave function $\phi(x, y)$ obeys the two-dimensional time-dependent Gross-Pitaevskii equation:

$$i\frac{\partial\phi}{\partial t} = \left[-\frac{1}{2}\nabla^2 + \frac{r^2}{2} + V_{\text{lat}} + U|\phi|^2 - \mu - \Omega L_z \right] \phi. \quad (1)$$

Unless otherwise specified we choose our units for time, length and energy as $1/\omega_{\perp}$, $\sqrt{\hbar/(m\omega_{\perp})}$ and $\hbar\omega_{\perp}$, respectively. Here $r^2 = x^2 + y^2$, U is the (renormalized) effective 2D nonlinear interaction coefficient, μ the chemical potential, L_z the z -component of the angular momentum operator, and $V_{\text{lat}} = V_0[\sin^2(kx) + \sin^2(ky)]$ is the optical lattice potential. In this work, we only consider the case where the optical lattice is co-rotating with the condensate, thus V_{lat} in Eq. (1) is time-independent.

For each chosen value of the OL periodicity (denoted by $a = \pi/k$), we vary the peak-to-peak potential amplitude of the optical lattice V_0 from 0 to V_{max} , a value at which the lattice is fully pinned. We obtain the ground state of the system for a given set of parameters (V_0, a, Ω) by propagating Eq. 1 in imaginary time (i.e. by steepest descent). To ensure that the obtained structure corresponds to the ground state, we usually start with several different initial trial wave functions possessing different symmetries for each set of parameters. In our calculation,

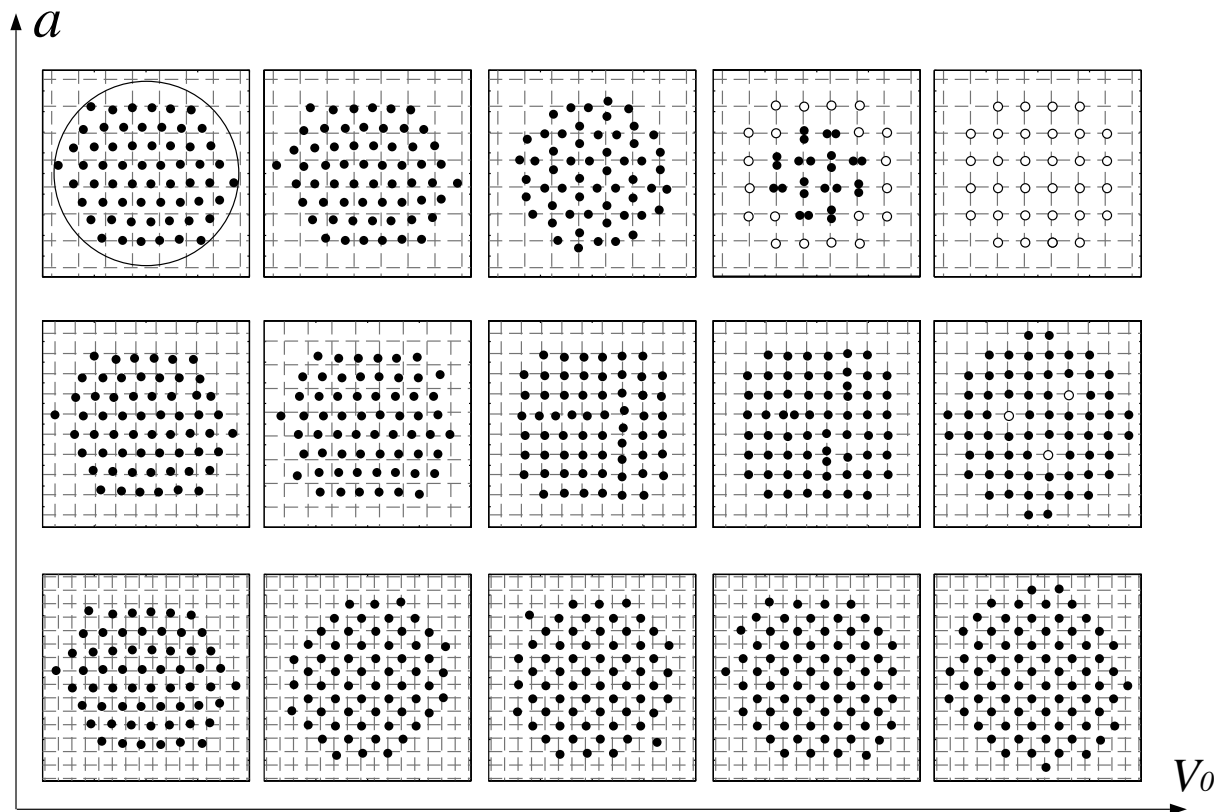


FIG. 1: Structure of the ground state. Each intersection of the dashed lines represents an antinode of the optical potential. Filled (●) and empty (○) circles represent the positions of singly and doubly quantized vortices, respectively. Only the positions of vortices within the Thomas-Fermi radius are shown. The Thomas-Fermi boundary $R_{TF} = \sqrt{2\mu}$ is represented by the circle in the upper-left plot. The upper, middle and lower rows correspond to $a = 4\epsilon/3$, ϵ and $2\epsilon/3$, or $\eta \approx 2$, 1.15 and 1/2, respectively. From left to right, $V_0 = 0.05$, 0.2, 0.5, 2.0 and 5.0, respectively.

we use the ^{87}Rb parameters of the JILA experiment [2]: $\omega_{\perp} = 2\pi \times 8.3\text{Hz}$, $\omega_z = 2\pi \times 5.3\text{Hz}$, $\Omega = 0.95\omega_{\perp}$, and the total particle number is taken to be 2×10^5 . Evidently, both the atomic and optical parameters will affect the ground state. For simplicity, in this work we focus on the effect resulting from variation of the OL. Our variables are therefore the depth (V_0) and periodicity (a) of the optical potential. Specifically, a defines the density of pinning sites which occur at the peaks of the OL potential whereas Ω determines the density of vortices. As found in previous studies [9], we observe that the structure of the fully pinned vortex lattice (FPVL) is very sensitive to the ratio η defined as $\eta = N_v/N_p$, where N_v and N_p are the density of vortices and pinning sites, respectively. For the OL potential we use here, $N_p = 1/a^2$. In the absence of the OL, $N_v = 2/(\sqrt{3}\epsilon^2)$, where $\epsilon = \sqrt{2\pi/(\sqrt{3}\Omega)}$ is the inter-vortex spacing in a completely unpinned ($V_0 = 0$) vortex lattice [11]. This value of N_v is not significantly changed by the presence of the OL. Hence we take $\eta \approx 2a^2/(\sqrt{3}\epsilon^2)$. In brief, we find that when $\eta \approx 1/2$, the FPVL has a checkerboard structure and when $\eta \approx 1$, we obtain a square lattice while when $\eta \approx 2$ we obtain a square lattice of doubly

charged vortices.

The trends in our results are graphically illustrated in Fig. 1, our main result. For three values of a the ground state vortex structure is plotted for increasing values of V_0 . The upper, middle and lower rows correspond to different pinning site densities represented by $a = 4\epsilon/3$, ϵ and $2\epsilon/3$, respectively. In this situation, the angular momentum of the condensate is carried in singly quantized vortices which organize into a triangular Abrikosov lattice due to the logarithmically repulsive inter-vortex interaction. Such vortex lattices have been observed [12], perturbed [2] and accurately described [13] by several groups in recent years.

As is not surprising, for sufficiently small V_0 the vortex lattice maintains a triangular geometry with only slight distortions (see first column of Fig. 1). In the opposite extreme, at sufficiently large values of V_0 , all the vortices are pinned to the antinodes of the OL potential, mirroring the geometry set by the OL potential. What is remarkable are the states that exist between these extremes. At $a = 4\epsilon/3$ (upper row of Fig. 1), there are about twice as many vortices as pinning sites ($\eta \approx 2$), and the FPVL is found to be a square lattice of doubly

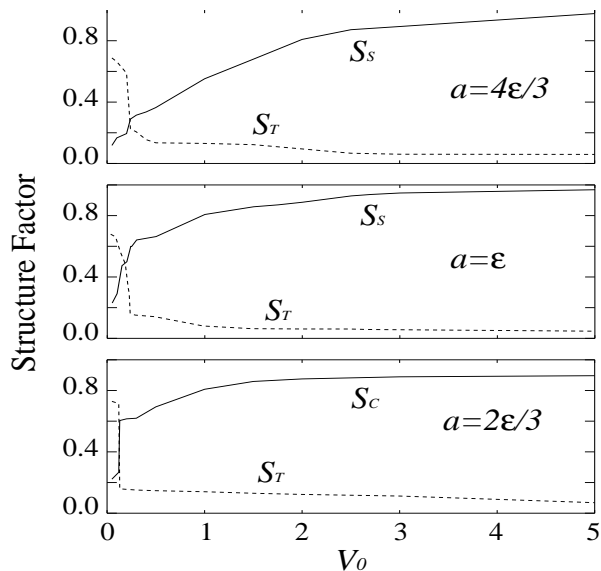


FIG. 2: Structure factors as functions of V_0 for $a = 4\epsilon/3$, ϵ and $2\epsilon/3$. $S_{T,S,C} = |S(\mathbf{k}_{T,S,C})|$, where $\mathbf{k}_{T,S,C} = (2\pi/\epsilon)\hat{x} - [2\pi/(\sqrt{3}\epsilon)]\hat{y}$, $2k\hat{y}$ and $k\hat{x} - k\hat{y}$, representing respectively one of the two fundamental reciprocal vectors for the triangular, square and checkerboard lattices.

quantized vortices which is commensurate with the OL, a situation analogous to the second matching field case for the superconductor system in which the observation of a square double-quanta vortex lattice was reported in Ref. [10]. At a higher pinning site density defined by $a = \epsilon$ (middle row of Fig. 1, $\eta \approx 1.15$), most of the antinodes of the OL are occupied by singly quantized vortices with the exception of three doubly quantized vortices. And finally, at $a = 2\epsilon/3$ (lower row of Fig. 1, $\eta \approx 1/2$), every next-nearest-neighbor site of the OL is occupied by a singly quantized vortex and the FPVL forms what can be described as a “checkerboard” square lattice rotated 45° with respect to the OL, once again analogous to the half matching field case of the superconductor system [9].

For intermediate values of V_0 , the vortices form structures in between the triangular lattice and the FPVL, the details of which also depend on the period of the OL. For example, at $a = 4\epsilon/3$, for which the FPVL is a square lattice of doubly charged vortices, we observe bound pairs centered around the OL pinning sites for the potential depth in the range $0.5 < V_0 < 4.0$. We point out that the orientation of each pair is orthogonal to all adjacent ones. As V_0 increases, these pairs are more and more tightly bound and eventually all pairs collapse onto the corresponding pinning sites thus forming doubly quantized vortices. Further increasing the OL period, vortices with higher and higher winding number will start to appear in the FPVL.

In order to characterize the SPT more quantitatively, we calculate the structure factor [9] of the vortex lattice

defined as:

$$S(\mathbf{k}) = \frac{1}{N_c} \sum_i n_i e^{i\mathbf{k}\cdot\mathbf{r}_i}, \quad (2)$$

where i labels individual vortices, n_i and \mathbf{r}_i are the winding number and position of the i -th vortex, while $N_c = \sum_i n_i$ is the total winding number. For a familiar crystal lattice, $|S(\mathbf{k})|$ displays peaks at the corresponding reciprocal lattice vectors. Here, we focus on following three cases: (1) the triangular Abrikosov lattice in the absence of the OL (S_T), (2) the square (S_S) and (3) the checkerboard (S_C) lattices defined by the OL. Each lattice structure has two fundamental reciprocal vectors. In this instance it is sufficient to calculate the structure factor along one dimension, i.e., for one of the reciprocal vectors. Our results are displayed in Fig. 2. We observe that as V_0 is increased from zero, the triangular lattice is destroyed over a very small range of V_0 as S_T exhibits a sudden jump, indicative of a first order transition which is physically expressed by the motion of vortices towards the pinning sites. When there are more vortices than pinning sites ($\eta > 1$), the surplus vortices get pinned at a comparatively “slow” pace as a consequence of repulsion experienced from vortices which are already pinned. Conversely, when the number of pinning sites exceeds that of vortices ($\eta < 1$), the FPVL is quickly established.

We now turn to explore the structure of the FPVL for various values of η . In the case η is not close to an integer or inverse integer value, we observe the coexistence of sub-lattices of different geometry bounded by domain walls which always lie along the diagonal of the OL. For $\eta = 1.8$ we have the coexistence of two sub-lattices formed by doubly and singly quantized vortices, respectively (see Fig. 3a). For this FPVL the domains have striped parallel walls (represented by the solid lines in the figure), indicating inter-domain repulsion [14, 15]. This can be understood as a consequence the repulsive vortex-vortex interaction. For the slightly smaller value of $\eta = 1.6$, these two sub-lattices form two interlocking checkerboard structure (see Fig. 3b). As a decreases further to 0.95ϵ (Fig. 3c), all doubly quantized vortices have disappeared and the vortex lattice becomes completely commensurate with the OL, with each pinning site hosting a singly quantized vortex. This represents the fully matching case of $\eta = 1$. Upon further decrease of a or η , Fig. 3d and e show that more pinning sites become unoccupied and the checkerboard domain begins to cover the whole lattice. In this ground state, the walls between the square and checkerboard domains are crossing each other, signifying an attractive domain wall interaction which may be intuitively understood as resulting from the tendency of the vortices to occupy the vacant pinning sites.

In the study of domain wall formation, we see again distinct advantages of BEC vortex lattices over alternative systems. Although similar domain formation was observed earlier in superconducting systems [10, 16], their origin could not be clearly established because of addi-

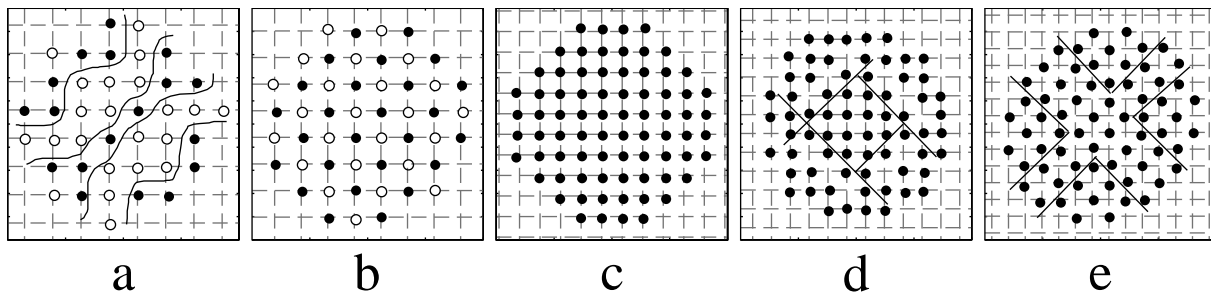


FIG. 3: Structure of the FPVL. From left to right, $\eta = 1.8, 1.6, 1.0, 0.8$ and 0.6 , corresponding to $a/\epsilon = 1.25, 1.176, 0.95, 0.833$ and 0.741 , respectively. Solid lines represent domain walls.

tional defects likely to be present in the experimental samples. By contrast, in the atomic BEC system, the OL provides us with a defect-free periodic pinning potential and thus frees us to confidently investigate the more fundamental factors controlling the dynamics of domain formation and hence the structure of the domain walls. Recent success at directly imaging [2] and calculating [13] vortex lattice excitations in BECs presents very exciting possibilities for studying, in unprecedented detail, the dynamics of the FPVLs obtained in this work and opens the door to more ambitious studies of SPTs in unconventional geometries.

In summary, we have theoretically investigated the vortex state of a rapidly rotating condensate in a periodic optical potential. We have found that the vortex lattice exhibits a rich variety of structures depending on the parameters of the optical potential. In the future it will be interesting to investigate the detailed dynamics (e.g. time evolution) of the phase transitions between various

structures and to relate the transitions to the properties of the condensate such as its collective excitation modes. Such studies will certainly shed new light on many other systems displaying structural phase transitions. In the current work, we have assumed that the optical potential is co-rotating with the condensate. We also plan to generalize this work to the case when the OL and the condensate are not co-rotating, under which condition, dynamical phases and phase transitions may exist [17].

This work is supported by the NSF, the ONR and the University of Rochester (LOB and NPB) and by Rice University (HP and SY). LOB is supported by the Laboratory for Laser Energetics Horton Program. NPB is also with the Institute of Optics. We thank Ennio Arimondo for fruitful discussions.

Note added—During the preparation of the paper, we noticed the work of Reijnders and Duine [18] who studied some aspects of this system using a variational approach.

-
- [1] K. A. Müller and H. Thomas (Ed.), *Structural Phase Transitions I and II* (Springer-Verlag, Berlin, New York, 1981, 1991); A. G. Khachatryan, *Theory of Structural Transformations in Solids* (Wiley, New York, 1983).
- [2] I. Coddington *et al.*, Phys. Rev. Lett. **91**, 100402 (2003); V. Schweikhard *et al.*, Phys. Rev. Lett. **92**, 040404 (2004).
- [3] D. Boiron *et al.*, Phys. Rev. A **57**, R4106 (1998); R. Dumke *et al.*, Phys. Rev. Lett. **89**, 097903 (2002); R. Newell, J. Sebby and T. G. Walker, Opt. Lett. **28**, 1266 (2003).
- [4] Z. Chen and K. McCarthy, Opt. Lett. **27**, 2019 (2002).
- [5] M. Greiner *et al.*, Nature (London) **415**, 39 (2002).
- [6] D. Jaksch *et al.*, Phys. Rev. Lett. **81**, 3108 (1998).
- [7] M. P. A. Fisher *et al.*, Phys. Rev. B **40**, 546 (1989).
- [8] K. Harada *et al.*, Science **274**, 5290 (1996); S. B. Field *et al.*, Phys. Rev. Lett. **88**, 067003 (2002); W. V. Pogosov, A. L. Rakhmanov and V. V. Moshchalkov, Phys. Rev. B **67**, 014532 (2003).
- [9] C. Reichhardt, C. J. Olson and F. Nori, Phys. Rev. B **57**, 7937 (1998); C. Reichhardt and N. Grønbech-Jensen, Phys. Rev. B **63**, 054510 (2001); C. Reichhardt *et al.*, Phys. Rev. B **64**, 144509 (2001).
- [10] A. N. Grigorenko *et al.*, Phys. Rev. B **63**, 052504 (2001).
- [11] A. L. Fetter and A. A. Svidzinsky, J. Phys. Condens. Matter **13**, R135 (2001).
- [12] K. W. Madison *et al.*, Phys. Rev. Lett. **84**, 806 (2000); J. R. Abo-Shaeer *et al.*, Science **292**, 476 (2001); P. C. Haljan *et al.*, Phys. Rev. Lett. **87**, 210403 (2001); E. Hodby *et al.*, Phys. Rev. Lett. **88**, 010405 (2002).
- [13] J. R. Anglin and M. Crescimanno, e-print cond-mat/0210063; G. Baym, Phys. Rev. Lett. **91**, 110402 (2003); L. O. Baksmaty *et al.*, Phys. Rev. Lett. **92**, 160405 (2004); T. Mizushima *et al.*, e-print cond-mat/0308010..
- [14] P. Bak *et al.*, Phys. Rev. B **19**, 1610 (1979).
- [15] K. Kern and G. Comsa, in *Chemistry and Physics of Solid Surfaces VII*, ed. by R. Vanselow and R. Howe (Springer, Berlin, Heidelberg 1988).
- [16] S. B. Field *et al.*, Phys. Rev. Lett. **88**, 067003 (2002).
- [17] G. Carneiro, Phys. Rev. B **66**, 054523 (2002).
- [18] J. W. Reijnders and R. A. Duine, preprint cond-mat/0401583.